Sains Malaysiana 53(8)(2024): 1953-1968
http://doi.org/10.17576/jsm-2024-5308-18

Synthesis, Molecular Docking and Heme Detoxification of Pyrano[2,3-c]pyrazole-aminoquinoline Hybrids as Potential Antimalarial Agents

(Sintesis, Dok Molekul dan Penyahtoksikan Hem Hibrid Pirano[2,3-c]pirazola-aminokuinolina sebagai Potensi Agen Antimalaria)

LEKKALA RAVINDAR[1], NG YAN HONG[2], KHAIRUL AZREENA BAKAR[2], AHMAD FADHLURRAHMAN BIN AHMAD HIDAYAT[3], SHEVIN RIZAL FEROZ[2], SAKI RAHEEM[4], SITI AISHAH HASBULLAH[1] & NURUL IZZATY HASSAN[1,*]

[1]Department of Chemical Sciences, Faculty of Science and Technology, Universiti Kebangsaan Malaysia, 43600 UKM Bangi, Selangor, Malaysia
[2]Department of Biological Sciences and Biotechnology, Faculty of Science and Technology,Universiti Kebangsaan Malaysia, 43600 UKM Bangi, Selangor, Malaysia
[3]Institute of Biological Sciences, Faculty of Science, Universiti Malaya, 50603 Kuala Lumpur, Malaysia[4]School of Life Sciences, University of Westminster, 115 New Cavendish Street, W1W 6UW, London, United Kingdom

Received: 11 March 2024/Accepted: 4 July 2024

ABSTRACT

Malaria, an infectious disease that spreads widely and can kill people, is still a problem for global health. This study adds to the list of possible solutions by making a group of new pyrano[2,3-c]pyrazole-aminoquinoline hybrids. Here, five novel hybrids were synthesized by covalently linking the scaffolds of 4-aminoquinoline and pyrano[2,3-c]pyrazoles *via* an ethyl linker. Molecular docking was used to study each hybrid's and standard chloroquine ability to bind to *Plasmodium falciparum* lactate dehydrogenase enzyme (*Pf*LDH), an important enzyme in the parasite's glycolytic pathway. The hybrid compounds had a stronger binding affinity than the standard chloroquine. Compound **4c** (-7.79 kcal/mol) and **4d** (-7.73 kcal/mol) had strong interactions with *Pf*LDH through hydrogen bonds, hydrophobic interactions, and Van der Waals interactions involving Val-26, Ile-54, Ala-98, Phe-100, Lys-118, Ile-119, and Glu-122. Additionally, the study explored the interaction between five hybrids and hemin, a pivotal component in the heme detoxification pathway of malaria parasites. The isothermal titration calorimetry (ITC) showed that the hybrids had different strengths when binding to hemin. This was because their structures were different. Hybrids **4a** and **4b** showed a strong affinity for hemin with *Ka* values of $(1.43 \pm 0.60) \times 10^6$ M^{-1} and $(1.64 \pm 0.97) \times 10^6$ M^{-1}, respectively, indicating that they might be able to stop the disruption process. In contrast, hybrids **4c**, **4d**, and **4e** interacted with hemin with markedly lower affinities. This study provides insights into the promising antimalarial properties of pyrano[2,3-c]pyrazole-aminoquinoline hybrids. It details their interactions with *Pf*LDH and hemin and offers potential avenues for developing novel therapeutic strategies against malaria.

Keywords: Isothermal titration calorimetry; Malaria; molecular docking; pyrano[2,3-c]pyrazole-aminoquinoline hybrids

ABSTRAK

Malaria, sejenis penyakit berjangkit yang merebak secara meluas dan membunuh manusia, masih menjadi masalah kesihatan global. Kajian ini mencari penyelesaian alternatif dengan menghasilkan kumpulan hibrid pirano[2,3-c]pirazola-aminokuinolina baharu. Lima sebatian hibrid baru telah disintesis dengan menghubungkan kerangka 4-aminokuinolina dan pirano[2,3-c]pirazola secara kovalen melalui penghubung etil. Pendokkan molekul digunakan untuk melihat keupayaan hibrid dan piawai klorokuina untuk mengikat enzim *Plasmodium falciparum* laktat dehidrogenase (*Pf*LDH), enzim penting dalam laluan glikolitik parasit. Sebatian hibrid menunjukkan pertalian pengikatan yang lebih kuat berbanding klorokuina piawai. Sebatian **4c** (-7.79 kcal/mol) dan **4d** (-7.73 kcal/mol) mempunyai interaksi yang kuat dengan *Pf*LDH melalui ikatan hidrogen, interaksi hidrofobik dan Van der Waals yang melibatkan asid amino Val-26, Ile-54, Ala-98, Phe-100, Lys-118, Ile-119 dan Glu-122. Selain itu, kajian ini meneroka interaksi antara lima hibrid dan hemin, komponen penting dalam laluan detoksifikasi hem parasit malaria. Kalorimetri titrasi isoterma (ITC) menunjukkan perbezaan kekuatan dalam ikatan hibrid terhadap hemin. Hal ini disebabkan struktur hibrid adalah berbeza. Hibrid **4a** dan **4b** memberikan keafinan yang kuat untuk hemin dengan nilai K_a $(1.43 \pm 0.60) \times 10^6$ M^{-1} dan $(1.64 \pm 0.97) \times 10^6$ M^{-1}, masing-masing, menunjukkan keupayaan perencatan. Sebaliknya, hibrid **4c**, **4d** dan **4e** berinteraksi dengan hemin dengan keafinan yang lebih rendah. Kajian ini

menunjukkan potensi antimalaria bagi hibrid pirano[2,3-c]pirazola-aminokuinolina. Interaksi dengan *Pf*LDH dan hemin secara lebih mendalam mampu membuka peluang untuk membangunkan strategi terapeutik baharu terhadap malaria.

Kata kunci: Hibrid pirano[2,3-c]pirazola-aminokuinolina; kalorimetri titrasi isoterma; malaria; pendokkan molekul

INTRODUCTION

One of the most common infectious diseases globally is malaria, which is transmitted through mosquito bites (Anopheles). *P. falciparum* causes the majority of malaria-related deaths (Greenwood et al. 2008; Hasan et al. 2015). It was the most frequent and deadly disease in 2021, killing 619000 people, mostly children and pregnant women (WHO Malaria Report 2022). To control malaria, diverse antimalarial drugs, for example, 4-aminoquinolines (chloroquine, hydroxychloroquine, piperaquine, and amodiaquine), 8-aminoquinolines (pamaquine, tafenoquine, aablaquine, and primaquine), 4-amino alcohols (quinine, quinidine, mefloquine, halofantrine, and lumefantrine), endoperoxides (artemisinin, dihydroartemisinin, artesunate, and artemether), antibiotics (doxycycline), antifolates (pyrimethamine, proguanil, and chloroproguanil), napthoquinones (atovaquone), sulfonamides (sulfadoxine and dapsone), and other antimalarial drugs have been used. The inevitable evolution of resistant strains of the malaria-causing parasite *Plasmodium* (Birkholtz et al. 2012; Tse, Korsik & Todd 2019) has led to a rise in the quest for novel drugs to treat malaria for the past ten years (Dorababu 2021; Kucharski, Jaszczak & Boratyński 2022; Qin et al. 2020; Ravindar et al. 2023c, 2022).

As the only standard treatment recommended by the WHO that exhibits comparable antimalarial resistance is artemisinin-based combination therapy (ACT), advancements in multi-therapeutic approaches have led to the development of analogues and the investigation of potential alternative pathways (Alven & Aderibigbe 2019; Tibon, Ng & Cheong 2020). Drug interactions can cause significant side effects, and developing a combination therapy that works effectively is expensive. Due to variations in pharmaceutical stability, pharmacokinetic properties, and solubility, choosing the proper drugs and dosages for combination therapy can be challenging. As a result, altering current drugs through the progress of hybrid molecules appears to be a potential approach (Raj, Land & Kumar 2015). The research groups of Meunier (2008) and Morphy (Morphy & Rankovic 2005) successfully developed the notion of hybrid molecules and hypothesized that they could potentially prevent the resurgence of drug resistance. Combination therapy can be overcome, and overall efficacy increased by molecular hybridization of two or more active pharmacophores into a single molecule (Singh et al. 2022; Szumilak & Wiktorowska-Owczarek & Stanczak 2021).

Chloroquine (CQ), a 4-aminoquinoline bicycle, has been highlighted as an effective antimalarial agent in the 21st century (Thomé et al. 2013; Uddin et al. 2021) due to its simple synthesis, simple usage, low cost, limited toxicity, and high clinical efficacy. Even though its clinical usage has been limited due to resistance, the 4-aminoquinoline moiety is crucial for delivering antimalarial efficiency by preventing haemozoin production and, as a result, accumulating the drug in the parasites' digestive vacuole (Zubir et al. 2022). Furthermore, a broad range of 4-aminoquinoline derivatives possessing superior antimalarial potency towards CQ-resistant *P. falciparum* strains have been reported (Ravindar et al. 2023a). This suggests that the resistance mechanism is likely compound-specific and is independent of alterations in the drug target's structure. Because of this, 4-aminoquinoline is still given particular consideration as a preferred scaffold in developing antimalarial drugs.

Pyrano[2,3-c]pyrazoles, another class of *N*-heterocycles, display diverse appealing biological activities, counting antimalarial activity (Biswas & Das 2022; García-Cañaveras et al. 2021; Shamsuddin et al. 2020; Witschel et al. 2015). Considering the broad range of therapeutic applications of pyranopyrazoles (Mandha et al. 2012; Ramiz et al. 2012; Wang et al. 2009) and 4-aminoquinolines (Abdi et al. 2021; Adeleke et al. 2021; Bekhit et al. 2022; Costa et al. 2020; Kaur & Kumar 2021; Li et al. 2023; Pawar et al. 2017; Ravindar et al. 2023b; Razzaghi-Asl et al. 2020; Shruthi et al. 2019), the hybridization of pyrano[2,3-*c*] pyrazoles with 4-aminoquinolines was envisaged to enhance the antimalarial efficacy of aminoquinoline-pyrano[2,3-*c*] pyrazole hybrid compounds. A successful procedure for conjugating 4-aminoquinoline and aliphatic/aromatic substituted pyrano[2,3-*c*]pyrazole compounds as a molecular hybrid of the antimalarial agent was recently reported by our research group (Shamsuddin et al. 2021). According to our previous results, the compounds with aliphatic or heterocyclic group on pyrano[2,3-c]pyrazole moiety have less impact on the antimalarial activity against CQ-sensitive or CQ-resistant strains, respectively. Hence, we furnished five new hybrid compounds by covalently linking the moieties of various aromatic substituted pyrano[2,3-c]pyrazoles and 4-aminoquinoline *via* an ethyl linker in this work.

These compounds were designed as potential antimalarial agents. Leveraging the historical significance of chloroquine, a widely used antimalarial drug, we selected it as a reference standard to examine the binding affinity of our novel hybrids with the *Pf*LDH enzyme through molecular docking studies. The three-dimensional structure of chloroquine served as a well-characterized ligand for validating our docking methods and parameters. Additionally, we conducted isothermal titration calorimetry

(ITC) experiments to experimentally determine the binding affinity of our synthesized hybrid compounds with hemin, a crucial component in the malaria parasite's heme metabolism. This integrated approach, combining computational and experimental techniques, aims to elucidate the potential antimalarial efficacy of our novel hybrid compounds and provide valuable insights into their mechanisms of action.

RESULTS AND DISCUSSION

SYNTHESIS OF PYRANO[2,3-C] PYRAZOLE-AMINOQUINOLINE HYBRIDS

The synthesis of various pyrano[2,3-c]pyrazole-aminoquinoline hybrid compounds was initiated by the synthesis of diverse pyrano[2,3-c]pyrazoles (**1a-1e**) through a one-pot four-component reaction of malononitrile, aldehyde, hydrazine and diethyl oxaloacetate in refluxing acidic ethanolic solution, employing acetic acid as a catalyst (Mohammat et al. 2018). Compared to the aromatic aldehyde with an electron-donating group (-OMe) at the *para* position (**1a**, 64%), the aldehydes containing electron-withdrawing chloro (**1b**, 74%), bromo (**1c**, 71%), and nitro (**1d**, 74%) groups at the same position had significantly higher yields. A lower yield (55%) was, however, observed in the case of *para*-hydroxy benzaldehyde (**1e**) (Scheme 1). On the other hand, the ethyl carbon chain was linked to the 4,7-chloroquinoline moiety by reacting to amino alcohol (ethanolamine) under neat conditions to provide 4-(ethanolamine)-7-chloroquine intermediate **2** with a much higher yield (94%) (Guantai et al. 2011). The intermediate **2** was then successfully converted to 4-(bromoethylamino)-7-chloroquinoline **3,** in moderate yield (70%) under established reaction conditions utilizing HBr-H_2SO_4 as brominating agent (Cazelles et al. 2011) (Scheme 1).

Having secured the synthesis of **1a-e** and **3**, the formation of intended pyrano[2,3-c]pyrazole-aminoquinoline hybrid compounds (**4a-4e)** was carried out by the hybridization of pyranopyrazole derivatives (**1a-e**) with 4-(bromoethylamino)-7-chloroquine (**3**) at 30-40 °C temperature under basic conditions, employing DMSO as a solvent (Shamsuddin et al. 2021). Compared to the other hybrids containing *para*-substituted (-Me, -Cl, -Br and -OH) phenyl ring on pyranopyrazole moiety, a higher yield was obtained in the case of hybrid **4d** (38%) containing a *para*-nitro substituted phenyl ring attached to the pyranopyrazole moiety (Scheme 1).

MOLECULAR DOCKING ANALYSIS

Molecular docking is a crucial computational tool in drug discovery, predicting the preferred orientation and binding affinity of small molecules or ligands within the active site of target proteins (Pinzi & Rastelli 2019). This *in silico* approach facilitates the identification and optimization of lead compounds by simulating molecular interactions between potential drug candidates and their target proteins. In this study, docking simulations were employed to predict the binding modes of CQ and a series of hybrid compounds to the cofactor binding site of the *Pf*LDH enzyme.

For the *Pf*LDH-CQ complex, the docking analysis showed 12 distinct conformation clusters (Figure 1(A)). The most populated cluster comprised 40 out of 100 conformations, with the conformation possessing the lower binding energy (–5.68 kcal/mol) belonging to this predominant cluster. Strikingly, the vast majority of the CQ conformations were distributed within a narrow range of binding energy, indicating the specific nature of the binding of CQ to *Pf*LDH. In contrast, the hybrid compounds were grouped into a greater number of distinct clusters (>34), which exhibited a relatively wide range of binding energies containing fewer ligand conformations (<18), as shown in Figure 1(B)–1(F). Notably, **4b-4e** exhibited a discrepancy between the cluster with the lower binding energy and the most populated cluster, suggesting that the most energetically favourable ligand configuration was not predominant during the simulations. However, the docking results showed that all the hybrids exhibited stronger.

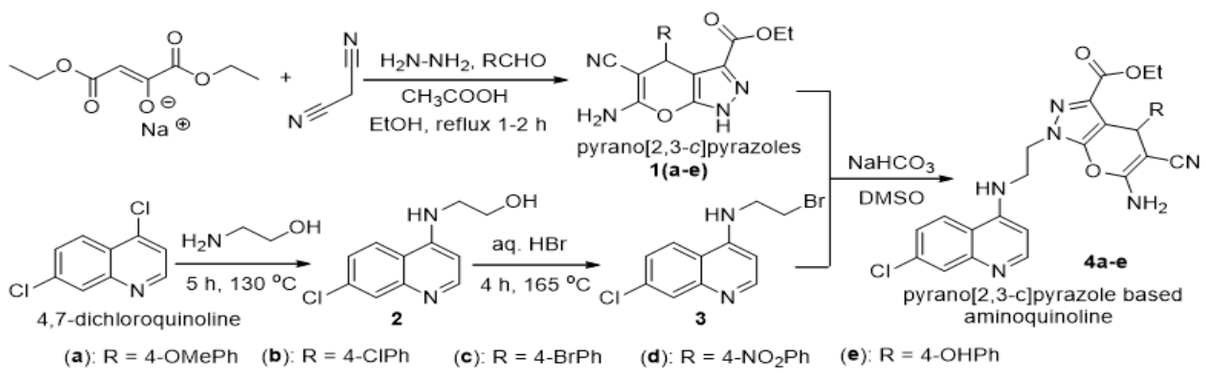

SCHEME 1. Synthesis of pyrano[2,3-c]pyrazole-aminoquinoline hybrids

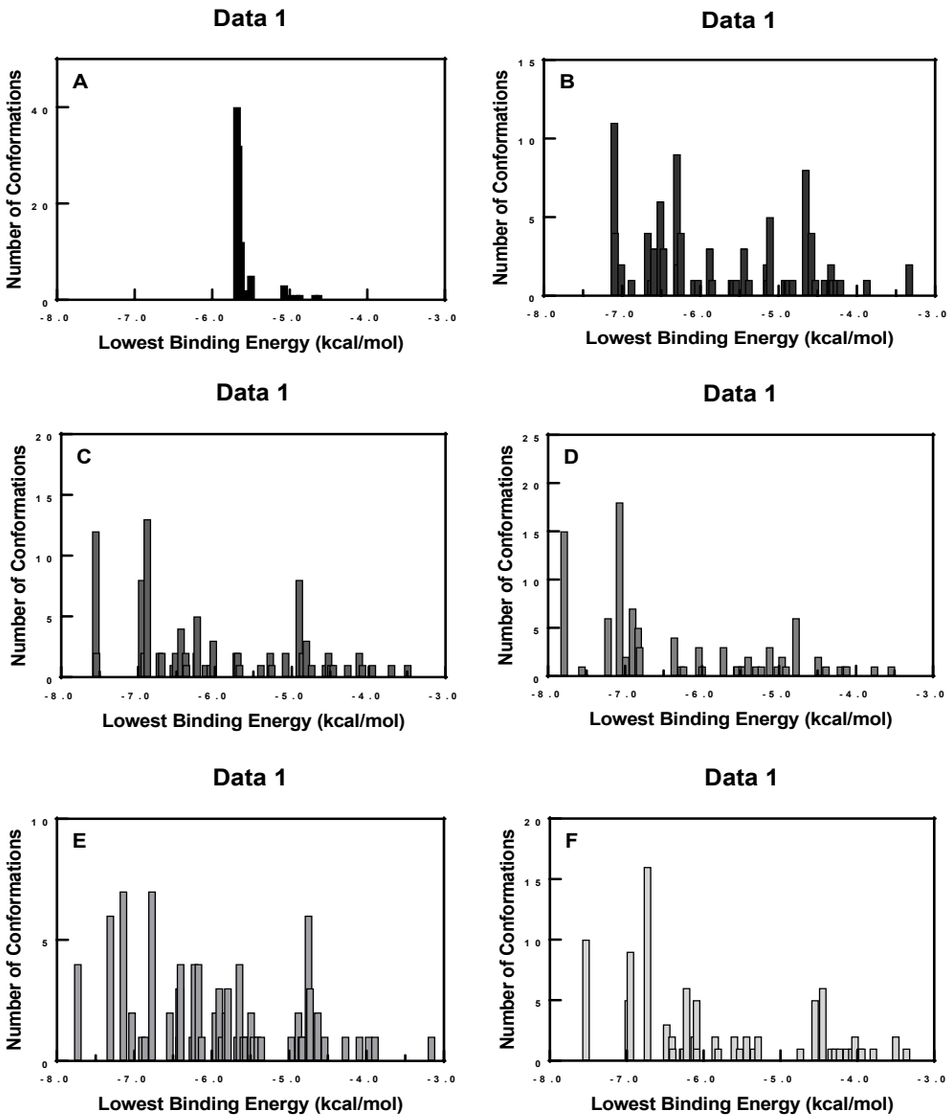

FIGURE 1. Cluster analysis of the docking of (A) CQ, (B) **4a**, (C) **4b**, (D) **4c**, (E) **4d**, and (F) **4e** to the cofactor binding site of *Pf*LDH (1CET), with outcomes generated from a total of 100 runs

binding to *Pf*LDH than CQ, with the lowest binding energies of <–7 kcal/mol. These findings imply that these compounds could form stable complexes with *Pf*LDH and strongly inhibit its enzymatic activity, thus, disrupting the energy metabolism of the malaria parasite.

The most stable ligand–*Pf*LDH complex for the above six compounds was then visualized and further examined, employing BIOVIA Discovery Studio Visualizer to determine the intermolecular interaction involved in the complexation (summarized in Table 1). The *Pf*LDH enzyme features a critical cofactor binding pocket encompassing key amino acid residues such as Val-26, Phe-52, Ile-54, Ala-98, Phe-100, Ile-119, and Glu-122 (Read et al. 1999; Zakaria, Lam & Hassan 2020).

For the CQ–*Pf*LDH complex (Figure 2), the formation of only a single hydrogen bond with Glu-122 was predicted. Thus, the stability of the interaction is significantly contributed by the collective presence of the various hydrophobic forces listed in Table 1. The π-σ interactions involved the association between the π electrons of CQ and the σ electrons of carbon-hydrogen (C-H) bonds in Ile-54, Ala-98, and Ile-119. Further, alkyl and π-alkyl interactions encompassed the nonpolar hydrophobic contacts between CQ and the alkyl groups of the amino acid residues at the binding site (Gómez-Jeria et al. 2020). Additionally, Van der Waals forces also partially contributed towards enhancing the stability of the complex.

TABLE 1. Intermolecular forces involved in *Pf*LDH (1CET) interactions with CQ and the **4a-4e** hybrids

Compound	Type of interaction	Bond type	Interacting residues
CQ	Hydrogen bond	Conventional	Glu-122
	Hydrophobic interaction	π-σ	Ile-54, Ala-98, Ile-119
		Alkyl	Ala-98, Ile-119
		π-alkyl	Val-26, Phe-52, Tyr-85, Lys-118
	Van der Waals forces		Gly-27, Asp-53, Phe-100, Ile-123
4a	Hydrogen bond	Conventional	Tyr-85
	Hydrophobic interaction	π-σ	Ile-119
		π-π T-shaped	Phe-100
		Alkyl	Ile-54, Phe-100
		π-alkyl	Ile-54, Phe-100, Leu-115, Lys-118
	Electrostatic interaction	π-anion	Glu-122
	Van der Waals forces		Val-26, Asp53, Ala-98, Ile123
4b	Hydrogen bond	Conventional	Tyr-85
		Carbon	Asp-53
	Hydrophobic interaction	π-σ	Ile-119
		Alkyl	Ile-54, Phe-100, Leu-115, Lys-118, Ile-119
		π-alkyl	Ile-54, Lys-118, Ile-119
	Electrostatic interaction	π-anion	Glu-122
	Van der Waals forces		Val-26, Ala-98, Leu-115, Ile-123
4c	Hydrogen bond	Conventional	Tyr-85
		Carbon	Asp-53
	Hydrophobic interaction	π-σ	Ile-119
		Alkyl	Ile-54, Phe-100, Leu-115, Ile-119
		π-alkyl	Ile-54, Leu-115, Lys-118
	Electrostatic interaction	π-anion	Glu-122
		π-cation	Lys-118
	Van der Waals forces		Val-26, Ala-98, Ile-123
4d	Hydrogen bond	Conventional	Gly-99, Lys-118, Glu-122 (2)
	Hydrophobic interaction	π-σ	Ile-119
		π-π T-shaped	Phe-100
		Alkyl	Ile-54, Tyr-85, Ala-98, Phe-100, Leu-115, Ile-119, Ile-123
		π-alkyl	Ile-54, Ala-98, Phe-100
	Van der Waals forces		Phe-52
4e	Hydrogen bond	Conventional	Tyr-85, Leu-115
		Carbon	Glu-122
	Hydrophobic interaction	π-σ	Ala-98
		π-π T-shaped	Phe-100
		Alkyl	Ile-54
		π-alkyl	Ile-54, Leu-115, Lys-118, Ile-119
	Van der Waals forces		Val-26, Gly-27, Phe-52, Asp-53, Asn-116, Ile-123

Compound **4c**, which possessed the lower docking energy, demonstrated a rich network of interactions with *Pf*LDH (Figure 3). These include conventional and carbon-hydrogens, with Tyr-85 and Asp-53, respectively (Tables 1). Unlike conventional hydrogen bonds, carbon-hydrogen bonds are comparatively weaker, characterized by a polarized carbon atom as the donor (Bulusu & Desiraju 2020). As with CQ, hydrophobic interactions due to alkyl, π-σ, and π-alkyl interactions were predicted to contribute to the overall stability of the **4c**–*Pf*LDH complexation. Interestingly, electrostatic forces are also involved, with both π-anion and π-cation interactions formed between the aromatic ring of the ligand and the charged residues Glu-122 and Lys-118, respectively. Although weaker than hydrogen bonding, their contributions towards stabilizing the complexation between **4c** and the protein should not be ignored (Infield et al. 2021; Plais et al. 2023). Together with the Van der Waals forces involving Val-26, Ala-98, and Ile-123, the various interactions described earlier have enhanced the system's stability, resulting in **4c** having the most energetically favourable interaction with *Pf*LDH.

Exhibiting the second lowest binding energy among the hybrids, **4d** formed a stable network of four hydrogen bonds with Gly-99, Lys-118, and Glu-122 (Figure 4), highlighting the importance of hydrogen bonding in its interaction with *Pf*LDH. Notably, there are no π-ion interactions with *Pf*LDH, as observed in the case of **4c**. Nevertheless, this is compensated by a π-π (T-shaped) interaction with Phe-100, in which the π-electron systems of two aromatic rings are arranged perpendicular to each other. Like the other hybrids, alkyl and π-alkyl interactions were pivotal in stabilizing the **4d**–*Pf*LDH complex; however, Van der Waals forces are less significant.

Meanwhile **4a**, **4b**, and **4e** exhibited relatively higher (less negative) binding energies than **4c** and **4d**, they still demonstrated favourable interactions with *Pf*LDH. Hydrogen bonds, hydrophobic contacts, electrostatic interactions (π-anion for **4a** and **4b**), and Van der Waals forces all contributed to the stability of the docked conformers. However, the absence of certain key interactions, as observed in **4c** and **4d,** may explain the slightly increased binding energies.

ISOTHERMAL TITRATION CALORIMETRY MEASUREMENTS

The interaction between the hybrids and hemin was examined by employing isothermal titration calorimetry (ITC) to evaluate their inhibition potential against heme detoxification. This technique measures the heat generated or absorbed during molecular binding events, which can be employed to quantify the binding affinity, K_a (Du et al. 2016). The ITC profiles of the interactions between hemin and compounds **4a-4e** are illustrated in Figure 5. As shown in Table 2, the K_a values of the hybrids ranged from 10^4 to 10^6 M^{-1}, with **4a** and **4b** exhibiting notably stronger affinity to hemin compared to compounds **4c-4e**. This variation in affinity towards hemin suggests distinct binding modes of the hybrids and sheds light on the structural nuances that influence the interactions of these compounds with hemin.

One mechanism of action of antimalarial drugs such as CQ, artemisinin, and their derivatives is binding to heme, which prevents the formation of heme crystals known as hemozoin. This leads to the accumulation of the toxic heme in the digestive vacuole, thus, killing the *Plasmodium* parasite (Wicht & Mok & Fidock 2020). Hence, the ability of compounds to bind favourably to heme can be used to evaluate their potential as antimalarial agents. Our results indicate that **4a** and **4b**, as distinguished by their strong heme binding affinity, could effectively disrupt the formation of hemozoin crystals and intervene in the heme detoxification process within the parasite. This information is valuable in understanding the molecular interactions involved in the action of antimalarial drugs and can be used to optimize the design of drug candidates for enhanced efficacy.

The thermodynamic parameters of the interactions are depicted in Table 2. All synthesized hybrid compounds exhibit exothermic reactions (negative ΔH), indicating heat release upon binding to hemin and forming intermolecular forces between the molecules. Furthermore, the entropy changes (ΔS) were negative for each interaction, implying a reduction in disorder resulting from hydrogen bonds and specific Van der Waals interactions constraining the molecules. The negative ΔG values reflect the spontaneity of these processes. Among the studied compounds, **4a** and **4b,** which showed the highest affinity towards hemin, also exhibited the most negative ΔG values, suggesting the most stable and favourable interactions with hemin. Interestingly, the interaction of the synthesized hybrids with hemin was enthalpy driven, as opposed to the entropy-driven binding of chloroquine to hematin (Vippagunta et al. 2000), presumably due to the additional pyrano[2,3-c]pyrazole group. These findings indicate that these compounds can effectively interact with heme and disrupt its detoxification in Plasmodium parasites, exerting antimalarial effects.

MATERIALS AND METHODS

All the solvents (ethyl acetate, n-hexane, toluene, dichloromethane, ethanol, methanol, and dimethyl sulfoxide) and chemicals used in this research were commercially available and did not require further purification. Activated charcoal (granulated), malononitrile 99%, hydrazine solution 35 wt.% in H_2O, diethyl oxalacetate sodium salt 95%, hydrobromic acid 48%, ethanolamine, 4,7-chloroquine 97%, acetic acid 98%, 4-methoxy benzaldehyde 99%, 4-chlorobenzaldehyde

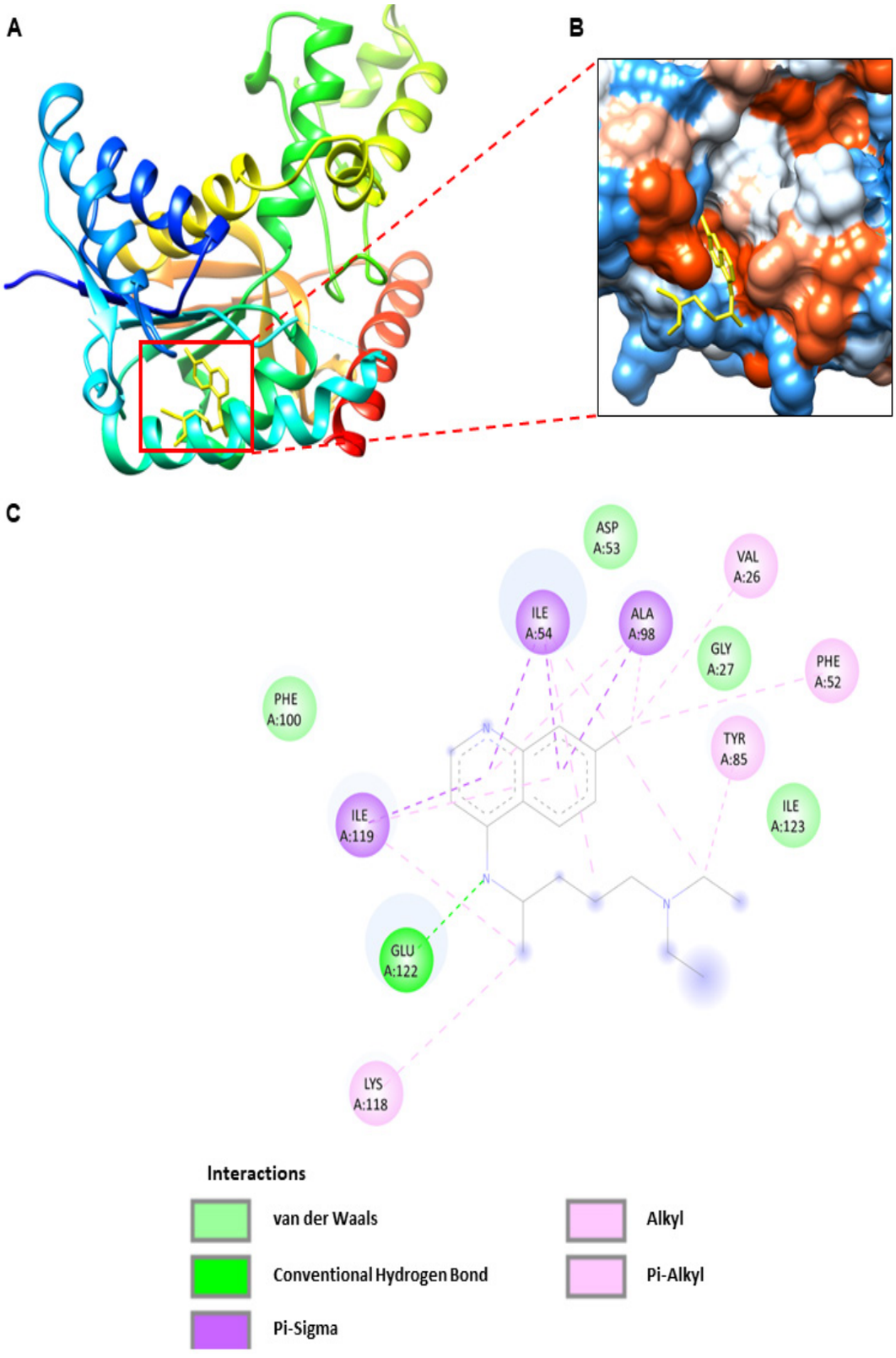

FIGURE 2. (A) Predicted orientation of the lower binding energy (–5.68 kcal/mol) conformation of CQ (rendered in ball and stick) on the *Pf*LDH enzyme. (B) Zoomed-in view of the cofactor binding site. (C) Schematic diagram of the intermolecular forces involved in the *Pf*LDH –CQ interaction

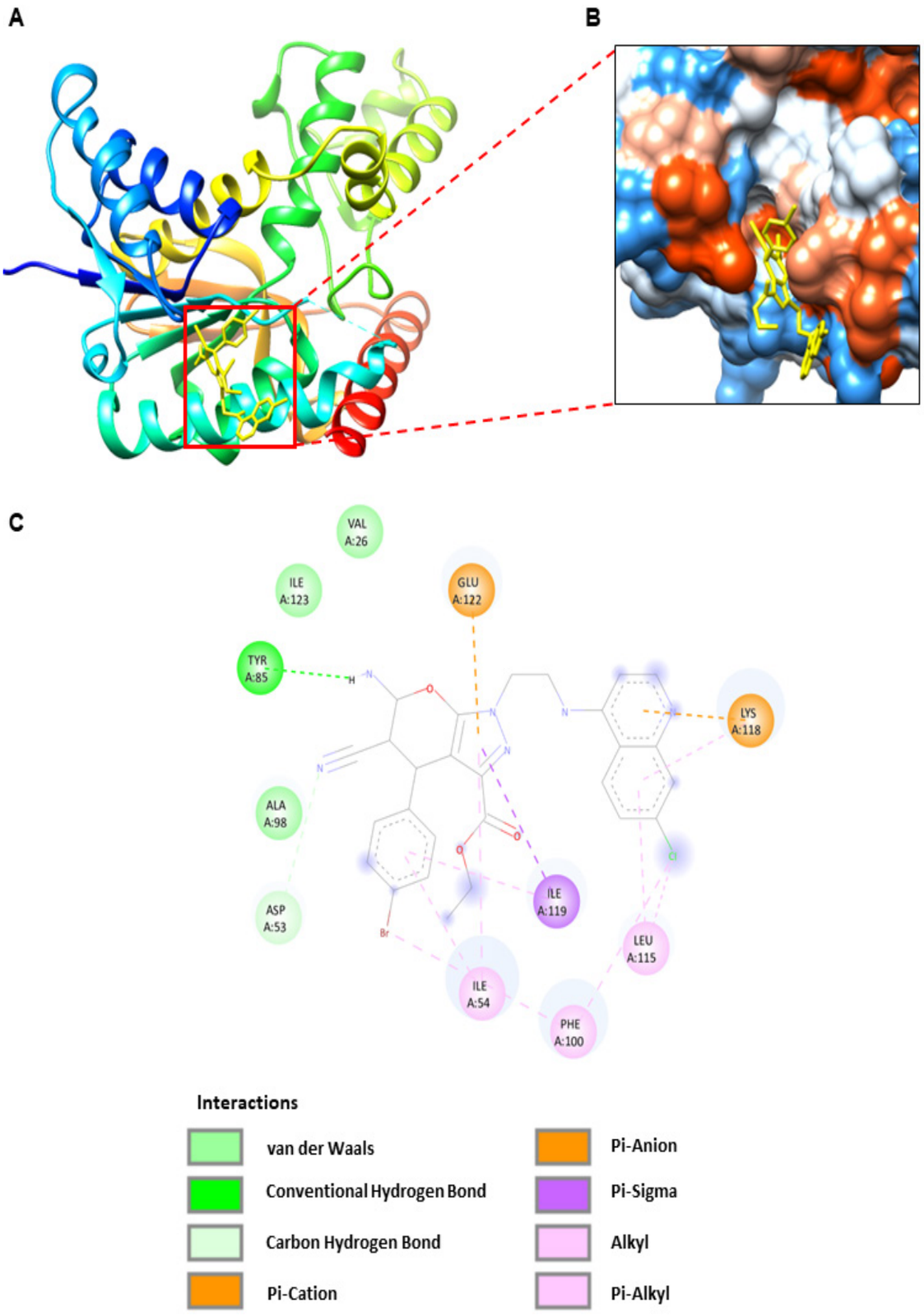

FIGURE 3. (A) Predicted orientation of the lower binding energy (–7.79 kcal/mol) conformation of **4c** (rendered in ball and stick) on the *Pf*LDH enzyme. (B) Zoomed-in view of the cofactor binding site. (C) Schematic diagram of the intermolecular forces involved in the *Pf*LDH –**4c** interaction

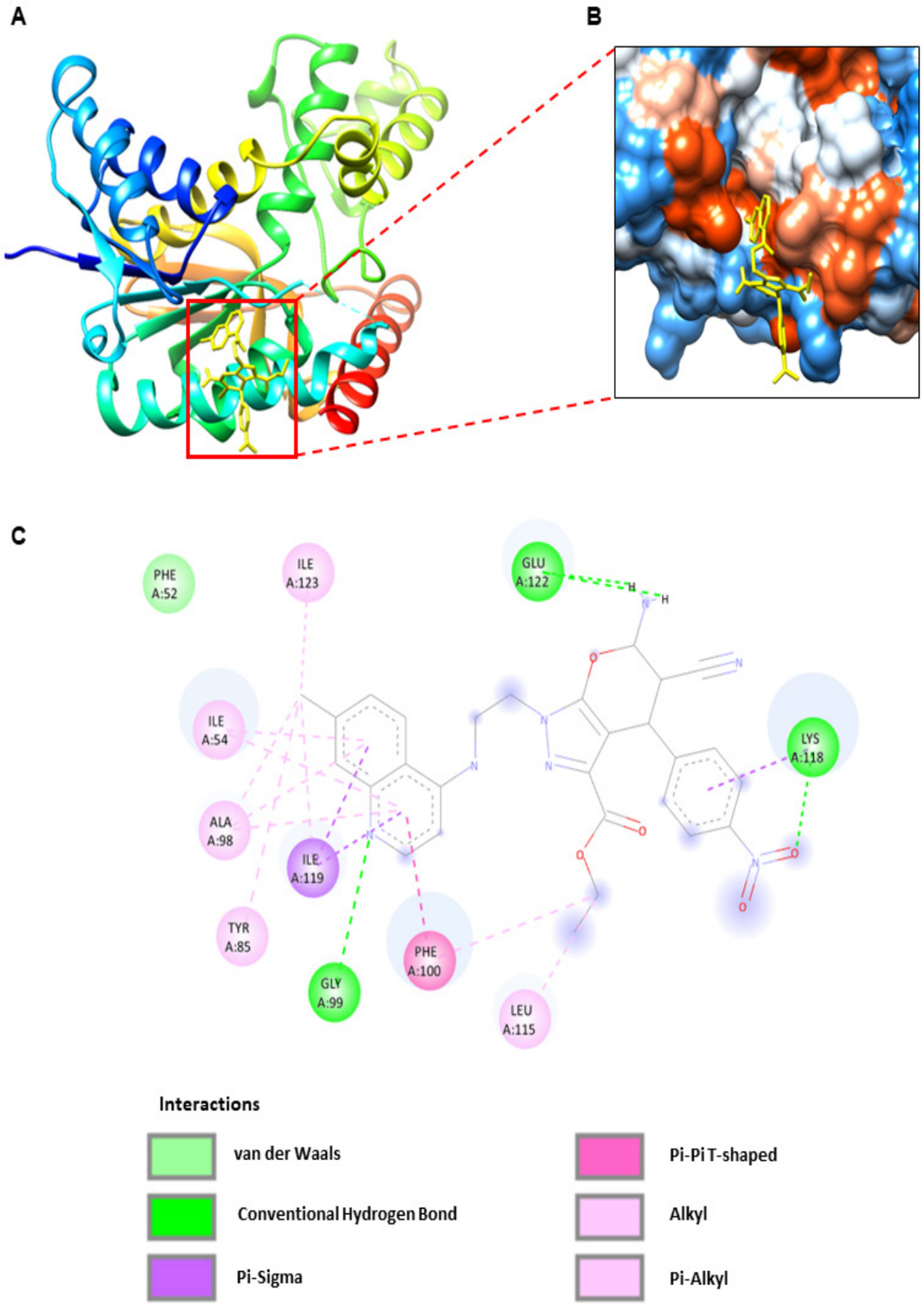

FIGURE 4. (A) Predicted orientation of the lower binding energy (–7.73 kcal/mol) conformation of **4d** (rendered in ball and stick) on the *Pf*LDH enzyme. (B) Zoomed-in view of the cofactor binding site. (C) Schematic diagram of the intermolecular forces involved in the *Pf*LDH –**4d** interaction

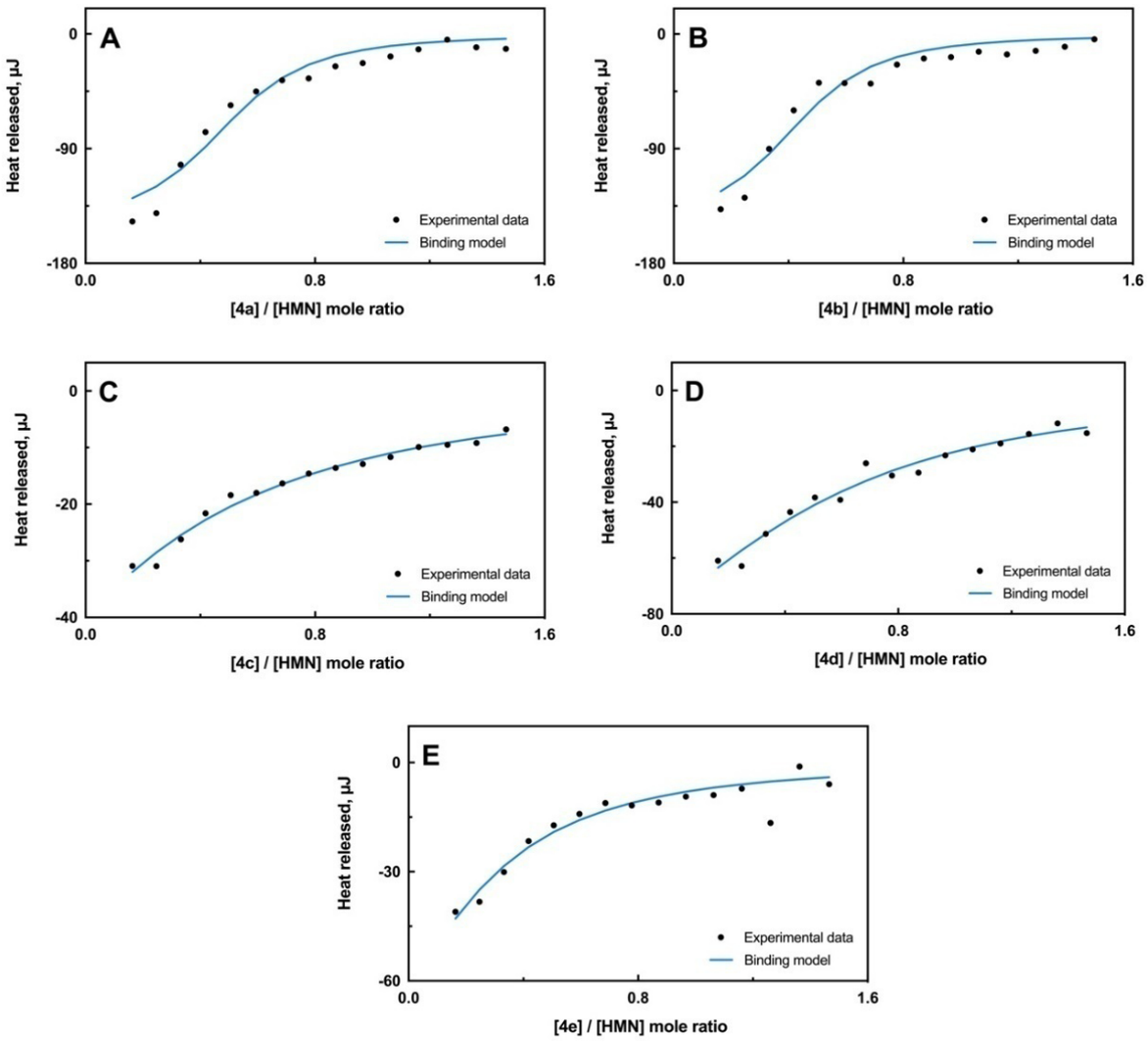

FIGURE 5. Isothermal titration calorimetric was obtained upon the titration of hemin with the different hybrids (A: **4a**, B: **4b**, C: **4c**, D: **4d**, and E: **4e**). The solid line represents the best fit to the measured heat values based on the independent binding model

TABLE 2. Binding affinity and thermodynamic parameters of the interaction between the synthesized hybrids and hemin at 37 °C, derived from ITC analysis

Complex	K_a (M^{-1})	$\triangle H$ (kJ mol^{-1})	$\triangle S$(J mol^{-1} K^{-1})	$\triangle G$ (kJ mol^{-1})
CQ–hematine	$(3.2\pm0.7)\times10^5$	50.208	-59.03	-32.64
4a–hemin	$(1.43\pm0.60)\times10^6$	(-71.66±6.68)	(-215.50±11.31)	(-36.83±0.79)
4b–hemin	$(1.64\pm0.97)\times10^6$	(-100 ± 0.00)	(-204.25±3.75)	(-36.64±1.16)
4c–hemin	$(7.45\pm3.42)\times10^4$	(-100 ± 0.00)	(-229.60±2.80)	(-28.79±0.87)
4d–hemin	$(3.37\pm3.54)\times10^5$	(-81.04±4.47)	(-203.48±17.20)	(-31.81±2.45)
4e–hemin	$(1.85\pm0.56)\times10^5$	(-96.55±3.45)	(-210.65±9.35)	(-31.21±0.56)

*(Mean ± standard deviation), CQ: chloroquine

97%, 4-bromobenzaldehyde 99%, 4-nitrobenzaldehyde 98%, and 4-hydroxybenzaldehyde 99% were purchased from Sigma-Aldrich, Darmstadt, Germany. Melting points were measured using the Stuart SMP40 instrument at room temperature till 300 °C. Elemental study was carried out by a Flash Elemental Analyzer 110 series (Selangor, Malaysia). The reaction progress was monitored using thin-layer chromatography (TLC) on Merck Kieselgel (New Jersey, NJ, USA) 60F254, which was visualized with an ultraviolet lamp, and the hybrids were purified utilizing silica gel column chromatography. ^{1}H and ^{13}C NMR spectra were recorded on a Joel Resonance ECZ400S 400 MHz spectrometer (Selangor, Malaysia) at 400 MHz and 100 MHz, respectively, with TMS as an internal standard in either *d6*-dimethyl sulphoxide (DMSO) or $CDCl_3$ solutions

General Procedure for the synthesis of Pyrano[2,3-c] pyrazoles (1a-e)

Pyrano[2,3-c]pyrazole compounds **1a-e** were furnished in good to better yields utilizing the procedure described by Mohammat et al. (2018). To a 100 mL oven-dried three-neck round-bottom flask with a stirring bar, added 5.5 mmol of diethyloxalacetate sodium salt, 1 mL acetic acid, 20 mL ethanol, and 5.5 mmol of 35% hydrazine solution. The reaction mixture was refluxed for 15 min. After adding 5 mmol of malononitrile and 5 mmol of carbonyl compound to the reaction mixture, it was vigorously refluxed for 30 min. The reaction mixture was cooled to room temperature once the reaction (monitored by TLC) was completed, and the precipitate formed was filtered out, washed with water, dried, and recrystallized from methanol.

SYNTHESIS OF ETHYL 6-AMINO-5-CYANO-4-(4-METHOXYPHENYL)-1,4-DIHYDROPYRANO[2,3-C] PYRAZOLE-3-CARBOXYLATE (1a)

Colorless solid (64%), m.p.: 235-236 °C; ^{1}H NMR (400 MHz, DMSO) δ 13.68 (s, 1H), 7.02-6.99 (m, 2H), 6.96 (s, 2H), 6.86-6.82 (m, 2H), 4.70 (s, 1H), 4.11 (q, *J* = 6.8 Hz, 2H), 3.71 (s, 3H), 1.10 (t, *J* = 6.8 Hz, 3H); ^{13}C NMR (75.5 MHz, DMSO): δ 160.4, 158.6, 158.4, 137.6, 130.4, 129.4, 128.8, 120.8, 114.9, 114.0, 104.5, 61.3, 58.7, 55.5, 36.7, 14.3.

SYNTHESIS OF ETHYL 6-AMINO-4-(4-CHLOROPHENYL)-5-CYANO-1,4-DIHYDROPYRANO[2,3-C]PYRAZOLE-3-CARBOXYLATE (1b)

Colorless solid (74%), m.p.: 228-230 °C; ^{1}H NMR (400 MHz, DMSO) δ 13.77 (s, 1H), 7.35 (dt, *J* = 9.2, 2.8 Hz, 2H), 7.13 (dt, *J* = 9.2, 2.4 Hz, 2H), 7.06 (s, 2H), 4.79 (s, 1H), 4.10 (q, *J* = 6.8 Hz, 2H), 1.07 (t, *J* = 6.8 Hz, 3H); ^{13}C NMR (75.5 MHz, DMSO): δ 160.5, 158.5, 156.0, 144.4, 131.6, 129.7, 129.6, 128.7, 120.6, 103.6, 61.4, 57.9, 36.8, 14.3.

SYNTHESIS OF ETHYL 6-AMINO-4-(4-BROMOPHENYL)-5-CYANO-1,4-DIHYDROPYRANO[2,3-C]PYRAZOLE-3-CARBOXYLATE (1c)

Colorless solid (71%), m.p.: 221-222 °C; ^{1}H NMR (400 MHz, DMSO) δ 13.77 (s, 1H), 7.49 (dt, *J* = 9.2, 2.4 Hz, 2H), 7.09-7.06 (m, 4H), 4.77 (s, 1H), 4.10 (q, *J* = 6.8 Hz, 2H), 1.07 (t, *J* = 6.8 Hz, 3H); ^{13}C NMR (75.5 MHz, DMSO): δ 160.5, 158.5, 156.0, 144.8, 131.6, 130.1, 129.6, 120.6, 120.1, 103.5, 61.4, 57.8, 36.9, 14.3.

SYNTHESIS OF ETHYL 6-AMINO-5-CYANO-4-(4-NITROPHENYL)-1,4-DIHYDROPYRANO[2,3-C] PYRAZOLE-3-CARBOXYLATE (1d)

Yellowish solid (74%), m.p.: 235-237 °C; ^{1}H NMR (400 MHz, DMSO) δ 13.85 (s, 1H), 8.18 (dt, *J* = 9.2, 2.4 Hz, 2H), 7.40 (dt, *J* = 9.6, 2.8 Hz, 2H), 7.18 (s, 2H), 4.97 (s, 1H), 4.08 (q, *J* = 7.2 Hz, 2H), 1.05 (t, *J* = 7.2 Hz, 3H); ^{13}C NMR (75.5 MHz, DMSO): δ 160.7, 158.4, 156.0, 152.7, 146.7, 129.8, 129.3, 124.1, 120.4, 102.8, 61.4, 57.1, 37.1, 14.3.

SYNTHESIS OF ETHYL 6-AMINO-5-CYANO-4-(4-HYDROXYPHENYL)-1,4-DIHYDROPYRANO[2,3-C] PYRAZOLE-3-CARBOXYLATE (1e)

Colorless solid (55%), m.p.: 217-218 °C; ^{1}H NMR (400 MHz, DMSO) δ 13.66 (s, 1H), 9.24 (s, 1H), 6.94 (s, 2H), 6.89 (dt, *J* = 9.6, 2.8 Hz, 2H), 6.66 (dt, *J* = 9.2, 2.8 Hz, 2H), 4.64 (s, 1H), 4.12 (q, *J* = 7.2 Hz, 2H), 1.10 (t, *J* = 7.2 Hz, 3H); ^{13}C NMR (75.5 MHz, DMSO): δ 160.3, 158.7, 156.4, 156.0, 135.9, 129.4, 128.7, 120.9, 115.4, 104.8, 61.3, 58.9, 36.7, 14.3.

SYNTHESIS OF 2-((7-CHLOROQUINOLIN-4-YL)AMINO) ETHAN-1-OL (2)

Aminoethanol (10 mL) and 4,7-dichloroquinoline (10 mmol) were added into a three-neck round-bottom flask and heated to 130 °C for five hours. After cooling to room temperature, the mixture was poured into cold water, where the compound precipitated. The precipitate was then filtered and vacuum-dried to produce 2-((7-chloroquinolin-4-yl)amino)ethan-1-ol (2) as a colorless solid with a 94% yield (Guantai et al. 2011).

Colorless solid (94%), m.p.: 210-211 °C; ^{1}H NMR (400 MHz, DMSO) δ 8.37 (d, *J* = 5.6 Hz, 1H), 8.26 (d, *J* = 8.8 Hz, 1H), 7.78 (d, *J* = 2 Hz, 1H), 7.45 (dd, *J* = 9.2, 2.4 Hz, 1H), 7.25 (t, *J* = 5.6 Hz, 1H), 6.51 (d, *J* = 5.2 Hz, 1H), 4.88 (s, 1H), 3.66 (s, 2H), 3.37 (t, *J* = 5.6 Hz, 2H); ^{13}C NMR (75.5 MHz, DMSO): δ 152.4, 150.7, 149.6, 133.8, 127.9, 124.5, 124.5, 117.9, 99.2, 59.2, 45.6.

SYNTHESIS OF N-(2-BROMOETHYL)-7-CHLOROQUINOLIN-4-AMINE (3)

Under cold (5-10 °C) conditions, 16.2 mmol of hydrobromic acid and then 5.5 mmol of sulphuric acid were added slowly to compound **2** (2.6 mmol).

TLC was used to monitor the reaction's progress while it refluxed for 4 h at 165 °C. The reaction mixture was quenched to adjust the pH to about 7 by gradually adding a $NaHCO_3$ solution. To obtain the corresponding product **3** in 70% yield as a colorless solid, the reaction mixture was extracted using dichloromethane, dried over Na_2SO_4, and concentrated under vacuum (Cazelles et al. 2011).
Colorless solid (70%), m.p.: 140-141 °C; ^{1}H NMR (400 MHz, DMSO) δ 8.44 (d, *J* = 5.2 Hz, 1H), 8.25 (d, *J* = 8.8 Hz, 1H), 7.82 (d, *J* = 2.4 Hz, 1H), 7.50 (dd, *J* = 9.2, 2.4 Hz, 1H), 6.59 (d, *J* = 5.6 Hz, 1H), 3.77-3.70 (m, 4H), 3.33 (s, 1H); ^{13}C NMR (75.5 MHz, DMSO): δ 151.8, 149.9, 146.4, 135.4, 125.7, 125.6, 124.8, 117.3, 99.4, 44.7, 31.6.

General Procedure for the Synthesis of Hybrid (4a–e)
Sodium bicarbonate (10 mmol) was added to a mixture of desired pyrano[2,3-c]pyrazole **1a–e** compounds (5 mmol) and 4-(bromoethylamino)-7-chloroquinoline (**3**, 5 mmol) in DMSO. The mixture was then vigorously stirred for 24 h at 30-40 °C. After cooling to room temperature, the mixture was extracted using 80 mL of brine and 20 mL of ethyl acetate. The organic layer was separated and then concentrated through a rotary evaporator. Finally, an ethyl acetate-hexane mixture (3:1) was used to purify all the synthesized hybrid compounds through silica column chromatography (Shamsuddin et al. 2021).

SYNTHESIS OF ETHYL 6-AMINO-1-(2-((7-CHLOROQUINOLIN-4-YL)AMINO)ETHYL)-5-CYANO-4-(4-METHOXYPHENYL)-1,4-DIHYDROPYRANO[2,3-C]PYRAZOLE-3-CARBOXYLATE (4a)
Brown solid (25%), m.p.: 169-171 °C; ^{1}H NMR (400 MHz, DMSO) δ 8.43 (d, *J* = 5.6 Hz, 1H), 8.10 (d, *J* = 9.2 Hz, 1H), 7.82 (d, *J* = 2 Hz, 1H), 7.48 (dd, *J* = 8.8, 2 Hz, 1H), 7.33 (dt, *J* = 9.6, 2.8 Hz, 1H), 7.01-6.99 (m, 2H), 6.91 (dt, *J* = 9.2, 2.8 Hz, 2H), 6.79 (dt, *J* = 9.2, 2.8 Hz, 2H), 6.55 (d, *J* = 5.6 Hz, 1H), 4.70-4.65 (m, 2H), 4.61 (s, 1H), 3.81 (s, 1H), 3.72 (s, 3H), 1.92 (s, 3H), 0.77 (t, *J* = 6.8 Hz, 3H); ^{13}C NMR (75.5 MHz, DMSO): δ 172.5, 161.4, 158.6, 158.3, 154.7, 137.4, 131.1, 128.6, 128.3, 124.6, 119.5, 117.3, 117.0, 114.2, 114.0, 105.9, 61.3, 58.8, 55.7, 55.5, 41.2, 37.0, 36.7, 24.1, 21.5, 13.7.

SYNTHESIS OF ETHYL 6-AMINO-4-(4-CHLOROPHENYL)-1-(2-((7-CHLOROQUINOLIN-4-YL)AMINO)ETHYL)-5-CYANO-1,4-DIHYDROPYRANO[2,3-C]PYRAZOLE-3-CARBOXYLATE (4b)
Pink solid (23%), m.p.: 157-159 °C; ^{1}H NMR (400 MHz, DMSO) δ 8.38 (d, *J* = 5.2 Hz, 1H), 8.06 (d, *J* = 9.2 Hz, 1H), 7.78 (d, *J* = 2.4 Hz, 1H), 7.48 (s, 1H), 7.37 (dd, *J* = 9.2, 2 Hz, 1H), 7.31 (d, *J* = 8.4 Hz, 2H), 7.05 (t, *J* = 8.8 Hz, 4H), 6.47 (d, *J* = 5.6 Hz, 1H), 4.71-4.62 (m, 3H), 3.71-3.60 (m, 4H), 0.69 (t, *J* = 6.8 Hz, 3H); ^{13}C NMR (75.5 MHz, DMSO): δ 160.1, 158.4, 154.7, 151.9, 150.3, 144.3, 134.0, 131.5, 129.7, 129.5, 128.7, 127.6, 124.7, 124.4, 120.5, 117.8, 104.9, 99.0, 61.2, 58.0, 49.7, 42.6, 37.1, 31.2, 13.6.

SYNTHESIS OF ETHYL 6-AMINO-4-(4-BROMOPHENYL)-1-(2-((7-CHLOROQUINOLIN-4-YL)AMINO)ETHYL)-5-CYANO-1,4-DIHYDROPYRANO[2,3-C]PYRAZOLE-3-CARBOXYLATE (4c)
Light pink solid (29%), m.p.: 171-173 °C; ^{1}H NMR (400 MHz, DMSO) δ 8.38 (d, *J* = 5.2 Hz, 1H), 8.00 (d, *J* = 9.2 Hz, 1H), 7.77 (d, *J* = 2 Hz, 1H), 7.44 (dt, *J* = 9.2, 2.4 Hz, 2H), 7.38-7.33 (m, 2H), 7.07 (s, 2H), 6.98 (dt, *J* = 9.2, 2.4 Hz, 2H), 6.48 (d, *J* = 5.6 Hz, 1H), 4.73-4.68 (m, 1H), 4.67 (s, 1H), 4.65-4.60 (m, 1H), 3.72-3.58 (m, 4H), 0.69 (t, *J* = 6.8 Hz, 3H); ^{13}C NMR (75.5 MHz, DMSO): δ 160.1, 158.4, 154.7, 152.2, 150.1, 149.4, 144.7, 133.9, 131.6, 129.9, 129.7, 127.8, 124.6, 124.2, 120.4, 120.0, 117.8, 104.8, 99.0, 61.2, 58.0, 49.7, 42.6, 37.2, 13.6.

SYNTHESIS OF ETHYL 6-AMINO-1-(2-((7-CHLOROQUINOLIN-4-YL)AMINO)ETHYL)-5-CYANO-4-(4-NITROPHENYL)-1,4-DIHYDROPYRANO[2,3-C]PYRAZOLE-3-CARBOXYLATE (4d)
Yellow solid (38%), m.p.: 198-200 °C; ^{1}H NMR (400 MHz, DMSO) δ 8.39 (d, *J* = 5.2 Hz, 1H), 8.13 (dt, *J* = 9.2, 2.4 Hz, 2H), 8.01 (d, *J* = 9.2 Hz, 1H), 7.76 (d, *J* = 2.4, 1H), 7.38-7.32 (m, 2H), 7.30 (dt, *J* = 9.6, 2.8 Hz, 2H), 7.18 (s, 2H), 6.47 (d, *J* = 5.6 Hz, 1H), 4.86 (s, 1H), 4.79-4.72 (m, 1H), 4.65-4.59 (m, 1H), 3.72-3.57 (m, 4H), 0.63 (t, *J* = 7.2 Hz, 3H); ^{13}C NMR (75.5 MHz, DMSO): δ 160.4, 158.2, 154.7, 152.7, 152.1, 150.1, 149.3, 146.6, 133.9, 129.9, 129.0, 127.8, 124.6, 124.2, 124.1, 120.2, 117.8, 104.0, 99.0, 61.3, 57.2, 49.8, 42.6, 37.4, 13.6.

SYNTHESIS OF ETHYL 6-AMINO-1-(2-((7-CHLOROQUINOLIN-4-YL)AMINO)ETHYL)-5-CYANO-4-(4-HYDROXYPHENYL)-1,4-DIHYDROPYRANO[2,3-C]PYRAZOLE-3-CARBOXYLATE (4e)
Light brown solid (19%), m.p.: 233-234 °C; ^{1}H NMR (400 MHz, DMSO) δ 9.26 (s, 1H), 8.38 (d, *J* = 5.6 Hz, 1H), 8.05 (d, *J* = 9.2 Hz, 1H), 7.79 (d, *J* = 2.4 Hz, 1H), 7.42 (dd, *J* = 9.2, 2.4 Hz, 1H), 6.94 (s, 2H), 6.82 (d, *J* = 8.4 Hz, 2H), 6.64 (d, *J* = 8.4 Hz, 2H), 6.47 (d, *J* = 5.6 Hz, 1H), 4.73-4.57 (m, 2H), 4.56 (s, 1H), 3.74-3.65 (m, 4H), 0.80 (t, *J* = 7.2 Hz, 3H); ^{13}C NMR (75.5 MHz, DMSO): δ 160.0, 158.7, 156.4, 154.7, 151.9, 150.4, 149.0, 135.8, 134.1, 129.5, 128.5, 127.6, 124.8, 124.3, 120.8, 117.8, 115.4, 106.1, 99.1, 61.3, 59.1, 49.7, 42.7, 37.0, 13.7.

MOLECULAR DOCKING

The X-ray crystallographic structure of *Pf*LDH was acquired from the Protein Data Bank (PDB ID: 1CET) with a resolution of 2.05 Å (Read et al. 1999). Initial 2D structures of all hybrid compounds were crafted using ChemDraw and subsequently transformed into 3D structures *via* Chem3D, with further refinement through energy minimization utilizing the MM2 force field. AutoDock Tools 1.5.7 (Sanner 1999) was utilized to make the protein and ligand structures for docking study. The protein crystal structure underwent the removal of ligands and water molecules to

serve as the docking receptor. Polar hydrogens were added, and Kollman united partial atom charges were assigned to the protein coordinates. Nonpolar hydrogens were merged for the ligands, rotatable bonds were defined, and Gasteiger charges were computed. Both protein and ligand data files were then converted into the pdbqt format for subsequent docking analysis.

The co-crystallized ligand, CQ, was first re-docked into the cofactor binding site of *Pf*LDH to examine the reliability of the docking process. All hybrid compounds (**4a-4e**) were docked at the same site. PyMOL (http://www.pymol.org/) and BIOVIA Discovery Studio Visualizer 4.5 (BIOVIA, Dassault Systèmes 2021) identified the amino acids present within this site. The docking coordinates were centred at x = 36.302, y = 11.09, and z = 19.234, with a box dimension of 40 × 40 × 40 points and 0.375 Å spacing. Molecular docking of the hybrid compounds to *Pf*LDH was executed using AutoDock 4.2 (Morris et al. 2009), employing the Lamarckian genetic algorithm search engine with 100 search runs and a population size of 150. Additional parameters were specified, including a maximum of 27000 generations, mutation rate of 0.02, crossover operator weight of 0.8, and elitism set at 1. Each ligand underwent 100 docking simulations and subsequent clustering analysis, with a root-mean-square deviation tolerance set at 2.0 Å. Upon completion, the most favourable docking conformation with the lowest binding energy was chosen for further examination to elucidate the binding energy and the intermolecular interactions involved using AutoDock Tools and BIOVIA Discovery Studio Visualizer, respectively.

ISOTHERMAL TITRATION CALORIMETRY

A Nano ITC microcalorimeter (TA Instruments, New Castle, DE, USA) was used to study the interaction between five hybrid compounds (**4a-4e**) and hemin at 37 °C. Stock solutions of the hybrids (2 mg/mL) were prepared by dissolution in DMSO, while a 0.5 mg/mL hemin solution was prepared in 0.5 M NaOH. These stock solutions were diluted with 10 mM sodium phosphate buffer, pH 7.4, while ensuring that the final samples contained 0.5 M NaOH and approximately 3% DMSO. Prior to the titration experiments, all samples were degassed under vacuum for 10 min. For the titration, 20 μM hemin was loaded into the sample cell, while the reference cell contained only deionized water. The hybrid compound (100 μM) was added to a 250 μL syringe and placed into the microcalorimeter. In order to guarantee complete mixing of the solutions, the titration technique comprised 16 repeated injections of 15 μL of the titrant into the sample cell, spaced 400 s apart. The stirring speed was kept at 200 rpm throughout. T Control tests were carried out by injecting the ligand into the buffer solution under comparable circumstances to account for the heat produced by solution mixing and dilution. The data obtained from these experiments were processed and analyzed using the NanoAnalyze software (v3.3.0), utilizing an independent binding model.

CONCLUSIONS

Several heme-binding antimalarial compounds that inhibit hemozoin formation have been discovered. Therefore, compounds that show heme detoxification results can be evaluated for their potential as antimalarial agents. In this study, five pyrano[2,3-c]pyrazole-aminoquinoline hybrids were successfully furnished and characterized using spectral analysis. Determination of the association constant (K_a) values from ITC experiments revealed varying affinities of the hybrids to hemin, reflecting the difference in their structures. Two hybrids, **4a** and **4b,** formed more stable interactions with hemin and are thus predicted to be better antimalarial candidates than the other three hybrids.

ACKNOWLEDGEMENTS

We thank Universiti Kebangsaan Malaysia for its financial assistance (UKM-TR2023-019) and for awarding the UKM Vice Chancellor Scholarship to Ravindar Lekkala.

REFERENCES

Abdi, B., Fekadu, M., Zeleke, D., Eswaramoorthy, R. & Melaku, Y. 2021. Synthesis and evaluation of the antibacterial and antioxidant activities of some novel chloroquinoline analogs. *Journal of Chemistry* 2021: 2408006.

Adeleke, A.A., Zamisa, S.J., Islam, M.S., Olofinsan, K., Salau, V.F., Mocktar, C. & Omondi, B. 2021. Quinoline functionalized schiff base silver (I) Complexes: Interactions with biomolecules and *in vitro* cytotoxicity, antioxidant and antimicrobial activities. *Molecules* 26(5): 1205.

Alven, S. & Aderibigbe, B. 2019. Combination therapy strategies for treating Malaria. *Molecules* 24(19): 3601.

Bekhit, A.A., Nasralla, S.N., El-Agroudy, E.J., Hamouda, N., El-Fattah, A.A., Bekhit, S.A., Amagase, K. & Ibrahim, T.M. 2022. Investigation of the anti-inflammatory and analgesic activities of promising pyrazole derivative. *European Journal of Pharmaceutical Sciences* 168: 106080.

Birkholtz, L.M., Bornman, R., Focke, W., Mutero, C. & de Jager, C. 2012. Sustainable malaria control: Transdisciplinary approaches for translational applications. *Malaria Journal* 11: 431.

Biswas, S.K. & Das, D. 2022. One-pot synthesis of pyrano[2,3-c] pyrazole derivatives via multicomponent reactions (MCRs) and their applications in medicinal chemistry. *Mini-Reviews in Organic Chemistry* 19: 552-568.

Bulusu, G. & Desiraju, G.R. 2020. Strong and weak hydrogen bonds in protein–ligand recognition. *Journal of the Indian Institute of Science* 100(1): 31-41.

Cazelles, J., Cosledan, F., Meunier, B. & Pellet, A. 2011. Dual molecules containing peroxy derivative, the synthesis and therapeutic applications thereof. https://patents.google.com/patent/US7947701B2/en

Costa, C.A., Lopes, R.M., Ferraz, L.S., Esteves, G.N.N., Di Iorio, J.F., Souza, A.A., de Oliveira, I.M., Manarin, F., Judice, W.A.S., Stefani, H.A. & Rodrigues, T. 2020. Cytotoxicity of 4-substituted quinoline derivatives: Anticancer and antileishmanial potential. *Bioorganic & Medicinal Chemistry* 28(11): 115511.

Dorababu, A. 2021. Quinoline: A promising scaffold in recent antiprotozoal drug discovery. *ChemistrySelect* 6(9): 2164-2177.

Du, X., Li, Y., Xia, Y-L., Ai, S-M., Liang, J., Sang, P., Ji, X-L. & Liu, S-Q. 2016. Insights into protein–ligand interactions: mechanisms, models, and methods. *International Journal of Molecular Sciences* 17(2): 144.

García-Cañaveras, J.C., Lancho, O., Ducker, G.S., Ghergurovich, J.M., Xu, X., da Silva-Diz, V., Minuzzo, S., Indraccolo, S., Kim, H., Herranz, D. & Rabinowitz, J.D. 2021. SHMT inhibition is effective and synergizes with methotrexate in T-cell acute lymphoblastic leukemia. *Leukemia* 35: 377-388.

Gómez-Jeria, J-S., Robles-Navarro, A., Kpotin, G., Gómez-Jeria, J.S., Kpotin, G.A., Garrido-Sáez, N. & Gatica-Díaz, N. 2020. Some remarks about the relationships between the common skeleton concept within the Klopman-Peradejordi-Gómez QSAR method and the weak molecule-site interactions. *Chemistry Research Journal* 5(2): 32-52.

Greenwood, B.M., Fidock, D.A., Kyle, D.E., Kappe, S.H., Alonso, P.L., Collins, F.H. & Duffy, P.E. 2008. Malaria: Progress, perils, and prospects for eradication. *Journal of Clinical Investigation* 11(4): 1266-1276.

Guantai, E.M., Ncokazi, K., Egan, T.J., Gut, J., Rosenthal, P.J., Bhampidipati, R., Kopinathan, A., Smith, P.J. & Chibale, K. 2011. Enone- and chalcone-chloroquinoline hybrid analogues: in silico guided design, synthesis, antiplasmodial activity, *in vitro* metabolism, and mechanistic studies. *Journal of Medicinal Chemistry* 54(10): 3637-3649.

Hasan, A., Mazumder, H.H., Chowdhury, A.S., Datta, A. & Khan, A. 2015. Molecular-docking study of malaria drug target enzyme transketolase in *Plasmodium falciparum* 3D7 portends the novel approach to its treatment. *Source Code for Biology and Medicine* 10: 7.

Infield, D.T., Rasouli, A., Galles, G.D., Chipot, C., Tajkhorshid, E. & Ahern, C.A. 2021. Cation-π interactions and their functional roles in membrane proteins. *Journal of Molecular Biology* 433(17): 167035.

Kaur, R. & Kumar, K. 2021. Synthetic and medicinal perspective of quinolines as antiviral agents. *European Journal of Medicinal Chemistry* 215: 113220.

Kucharski, D.J., Jaszczak, M.K. & Boratyński, P.J. 2022. A review of modifications of quinoline antimalarials: Mefloquine and (hydroxy)chloroquine. *Molecules* 27(3): 1003.

Li, Z-H., Yin, L-Q., Zhao, D-H., Jin, L-H., Sun, Y-J. & Tan, C. 2023. SAR studies of quinoline and derivatives as potential treatments for Alzheimer's disease. *Arabian Journal of Chemistry* 16: 104502.

Loeb, F., Clark, W.M., Coateny, G.R., Coggeshall, L.T., Dieuaide, F.R., Dochez, A.R., Hankansson, E.G., Marshall Jr., E.K., Marvel, C.S., McCoy, O.R., Sapero, J.J., Sebrell, W.H., Shannon, J.A. & Carden Jr., G.A. 1946. Activity of a new antimalarial agent, chloroquine (SN 7618): Statement approved by the board for coordination of malarial studies. *Journal of the American Medical Association* 130: 1069.

Mandha, S.R., Siliveri, S., Alla, M., Bommena, V.R., Bommineni, M.R. & Balasubramanian, S. 2012. Eco-friendly synthesis and biological evaluation of substituted pyrano[2,3-c]pyrazoles. *Bioorganic & Medicinal Chemistry Letters* 22(16): 5272-5278.

Meunier, B. 2008. Hybrid molecules with a dual mode of action: Dream or reality? *Accounts of Chemical Research* 41(1): 69-77.

Mohammat, M.F., Maarop, M.S., Shaameri, Z., Wibowo, A., Johari, S.A. & Hamzah, A.S. 2018. Practical synthesis and electronic study of non-spiro and spiropyrano[2,3-c]pyrazole-3-carboxyate derivatives via uncatalyzed domino one-pot, four-component reactions. *Organic Communications* 11: 149-162.

Morphy, R. & Rankovic, Z. 2005. Designed multiple ligands. An emerging drug discovery paradigm. *Journal of Medicinal Chemistry* 48(21): 6523-6543.

Morris, G.M., Huey, R., Lindstrom, W., Sanner, M.F., Belew, R.K., Goodsell, D.S. & Olson, A.J. 2009. AutoDock4 and AutoDockTools4: Automated docking with selective receptor flexibility. *Journal of Computational Chemistry* 30(16): 2785-2791.

Pawar, P., Mane, B., Salve, M. & Bafana, S. 2017. Synthesis and anticonvulsant activity of n-substituted-7-hydroxy-4-methyl- 2-oxa-quinoline derivatives. *International Journal of Drug Research and Technology* 3(3): 60-66.

Pinzi, L. & Rastelli, G. 2019. Molecular docking: Shifting paradigms in drug discovery. *International Journal of Molecular Sciences* 20(18): 4331.

Plais, R., Clavier, G., Salpin, J., Gaucher, A. & Prim, D. 2023. Anion-π interaction for molecular recognition of anions: Focus on cooperativity with hydrogen bonding. *European Journal of Organic Chemistry* 26(9): e202201281.

Qin, H-L., Zhang, Z-W., Lekkala, R., Alsulami, H. & Rakesh, K.P. 2020. Chalcone hybrids as privileged scaffolds in antimalarial drug discovery: A key review. *European Journal of Medicinal Chemistry* 193: 112215.

Raj, R., Land, K.M. & Kumar, V. 2015. 4-Aminoquinoline-hybridization en route towards the development of rationally designed antimalarial agents. *RSC Advances* 5(101): 82676-82698.

Ramiz, M.M.M., Hafiz, I.S.A., Rahim, M.A.M.A. & Gaber, H.M. 2012. Pyrazolones as building blocks in heterocyclic synthesis: Synthesis of new pyrazolopyran, pyrazolopyridazine and pyrazole derivatives of expected antifungicidal activity. *Journal of the Chinese Chemical Society* 59(1): 72-80.

Ravindar, L., Hasbullah, S.A., Rakesh, K.P. & Hassan, N.I. 2023a. Recent developments in antimalarial activities of 4-aminoquinoline derivatives. *European Journal of Medicinal Chemistry* 256: 115458.

Ravindar, L., Hasbullah, S.A., Rakesh, K.P., Raheem, S., Agustar, H.K., Ismail, N., Ling, L.Y. & Hassan, N.I. 2023b. Exploring diverse frontiers: Advancements of bioactive 4-aminoquinoline-based molecular hybrids in targeted therapeutics and beyond. *European Journal of Medicinal Chemistry* 264: 116043.

Ravindar, L., Hasbullah, S.A., Rakesh, K.P. & Hassan, N.I. 2023c. Triazole hybrid compounds: A new frontier in malaria treatment. *European Journal of Medicinal Chemistry* 259: 115694.

Ravindar, L., Hasbullah, S.A., Rakesh, K.P. & Hassan, N.I. 2022. Pyrazole and pyrazoline derivatives as antimalarial agents: A key review. *European Journal of Pharmaceutical Science* 183: 106365.

RazzaghiAsl, N., Sepehri, S., Ebadi, A., Karami, P., Nejatkhah, N. & JohariAhar, M. 2020. Insights into the current status of privileged Nheterocycles as antileishmanial agents. *Molecular Diversity* 24: 525-569.

Read, J.A., Wilkinson, K.W., Tranter, R., Sessions, R.B. & Brady, R.L. 1999. Chloroquine binds in the cofactor binding site of *Plasmodium falciparum* lactate dehydrogenase. *The Journal of Biological Chemistry* 274(15): 10213-10218.

Sanner, M.F. 1999. Python: A programming language for software integration and development. *Journal of Molecular Graphics & Modelling* 17(1): 57-61.

Shamsuddin, M.A., Ali, A.H., Zakaria, N.H., Mohammat, M.F., Hamzah, A.S., Shaameri, Z., Lam, K.W., Mark-Lee, W.F., Agustar, H.K., Mohd Abd Razak, M.R., Latip, J. & Hassan, N.I. 2021. Synthesis, molecular docking, and antimalarial activity of hybrid 4-aminoquinoline-pyrano[2,3-c]pyrazole derivatives. *Pharmaceuticals* 14: 1174-1190.

Shamsuddin, M.A., Zakaria, N.H., Mohammat, M.F., Syahri, J., Latip, J. & Hassan, N.I. 2020. Synthesis and molecular docking studies of pyrano[2,3-c] pyrazole-3-carboxylates as potential inhibitors of *Plasmodium falciparum*. *Malaysian Journal of Chemistry* 22: 52-61.

Shruthi, T.G., Eswaran, S., Shivarudraiah, P., Narayanan, S. & Subramanian, S. 2019. Synthesis, antituberculosis studies and biological evaluation of new quinoline derivatives carrying 1,2,4-oxadiazole moiety. *Bioorg. Bioorganic & Medicinal Chemistry Letters* 29(1): 97-102.

Singh, A.K., Kumar, A., Singh, H., Sonawane, P., Paliwal, H., Thareja, S., Pathak, P., Grishina, M., Jaremko, M., Emwas, A.H., Pal Yadav, J., Verma, A., Khalilullah, H. & Kumar, P. 2022. Concept of hybrid drugs and recent advancements in anticancer hybrids. *Pharmaceuticals* 15(9): 1071.

Szumilak, M., Wiktorowska-Owczarek, A. & Stanczak, A. 2021. Hybrid drugs-A strategy for overcoming anticancer drug resistance? *Molecules* 26(9): 2601.

Thomé, R., Lopes, S.C.P., Costa, F.T.M. & Verinaud, L. 2013. Chloroquine: Modes of action of an undervalued drug. *Immunology Letters* 153(1-2): 50-57.

Tibon, N.S., Ng, C.H. & Cheong, S.L. 2020. Current progress in antimalarial pharmacotherapy and multi-target drug discovery. *European Journal of Medicinal Chemistry* 188: 111983.

Tse, E.G., Korsik, M. & Todd, M.H. 2019. The past, present and future of antimalarial medicines. *Malaria Journal* 18: 93.

Vippagunta, S.R., Dorn, A., Ridley, R.G. & Vennerstrom, J.L. 2000. Characterization of chloroquine-hematin W-oxo dimer binding by isothermal titration calorimetry. *Biochimica et Biophysica Acta* 1475: 133-140.

Wang, J.L., Liu, D., Zheng, Z.J., Shan, S., Han, X., Srinivasula, S.M., Croce, C.M., Alnemri, E.S. & Huang, Z. 2009. Structure-based discovery of an organic compound that binds Bcl-2-protien and induces apoptosis of tumor cell. *Proceedings of the National Academy of Sciences of the United States of Americ*a 97(13): 7124-7129.

Uddin, A., Chawla, M., Irfan, I., Mahajan, S., Singh, S. & Abid, M. 2021. Medicinal chemistry updates on quinoline- and endoperoxide-based hybrids with potent antimalarial activity. *RSC Medicinal Chemistry* 12: 24-42.

Wicht, K.J., Mok, S. & Fidock, D.A. 2020. Molecular mechanisms of drug resistance in *Plasmodium falciparum* malaria. *Annual Review of Microbiology* 74(1): 431-454.

Witschel, M.C., Rottmann, M., Schwab, A., Leartsakulpanich, U., Chitnumsub, P., Seet, M., Tonazzi, S., Schwertz, G., Stelzer, F., Mietzner, T., McNamara, C., Thater, F., Freymond, C., Jaruwat, A., Pinthong, C., Riangrungroj, P., Oufir, M., Hamburger, M., Mäser, P., Sanz-Alonso, L.M., Charman, S., Wittlin, S., Yuthavong, Y., Chaiyen, P. & Diederich, F. 2015. Inhibitors of plasmodial serine hydroxymethyltransferase (SHMT): Cocrystal structures of pyrazolopyrans with potent blood- and liver-stage activities. *Journal of Medicinal Chemistry* 58: 3117-3130.

WHO Malaria Report. 2022. http://www.who.int/teams/globalmalariaprogramme/reports/world-malaria-report-2022 (Accessed in February 2023).

Zakaria, N.H., Lam, K.W. & Hassan, N.I. 2020. Molecular docking study of the interactions between *Plasmodium falciparum* lactate dehydrogenase and 4-aminoquinoline hybrids. *Sains Malaysiana* 49(8): 1905-1913.

Zubir, N.M., Abd Razak, M.R.M., Ali, A.H., Mackeen, M.M. & Hassan, N.I. 2022. Konsep penghibridan 4-aminokuinolina sebagai alternatif agen antiplasmodium. *Sains Malaysiana* 51(10): 3463-3479.

*Corresponding author; email: drizz@ukm.edu.my